Available online at www.sciencedirect.com
ScienceDirect
Ceramics International 34 (2008) 1487–1494
CERAMICS INTERNATIONAL
www.elsevier.com/locate/ceramint

Shrinkage behavior and interfacial diffusion in Ni-based internal electrodes with $BaTiO_3$ additive

Ji-Hun Kang [a], Dongwon Joo [a], Hyun-Min Cha [a], Yeon-Gil Jung [a,*], Ungyu Paik [b]

[a] School of Nano & Advanced Materials Engineering, Changwon National University, 9 Sarim-dong, Changwon, Kyungnam 641-773, Republic of Korea
[b] Division of Advanced Materials Engineering, Hanyang University, 17 Haengdang-dong, Seongdong-gu, Seoul 133-791, Republic of Korea

Received 22 August 2006; received in revised form 20 March 2007; accepted 4 April 2007
Available online 10 May 2007

Abstract

The effects of particle size of starting materials and amount of a $BaTiO_3$ additive on the shrinkage behavior and elemental diffusion in Ni-based internal electrodes have been investigated in order to control the shrinkage of the internal electrode in multilayer ceramic capacitors (MLCCs). Two kinds of Ni and $BaTiO_3$ powders were used with different particle sizes. Volume shrinkage over the range of 700–1300 °C at 150 °C intervals and linear shrinkage during sintering were measured for starting materials and composites in a reducing atmosphere. The interfaces of Ni/$BaTiO_3$ composites with 90:10 and 70:30 volume ratios, respectively, were investigated using TEM. Composites with bimodal Ni powder show less shrinkage than those with monomodal Ni powder, showing less shrinkage in monolith Ni of bimodal particle size. The shrinkage behavior is changed during sintering with increasing amounts of $BaTiO_3$ additives in both Ni-based composites. The particle size of the $BaTiO_3$ additive affects the shrinkage behavior of composites, without the additional amount affecting the final shrinkage. A reaction layer of about 300 nm wide is observed at the interface between the Ni and $BaTiO_3$ powders in composites, in which elemental Ni diffuses into the $BaTiO_3$ without counterdiffusion.

Keywords: B. Interfaces; C. Diffusion; E. Capacitors; Internal electrode

1. Introduction

In the fabrication process for multilayer ceramic capacitors (MLCCs), the downsizing of dielectric and internal electrode layers and the reducing of cost are key processing technologies to meet the demand for miniaturization of electric components and to improve properties. For this purpose, smaller-sized powders and cheaper base metals need to be used as dielectric and electrode materials, respectively, and more attention must be given to the sintering process to control the shrinkage mismatch between dielectric and electrode layers in MLCCs, as this is the main reason for residual stress resulting in cracking and delamination during fabrication and service [1–6].

A significant number of residual pores are formed after binder burnout, giving a porosity of 40–50 vol.%. Even though the residual pores disappear during the sequential sintering process, normally the sintering process shows a shrinkage mismatch, larger than a 10% linear shrinkage ratio, between the ceramics and the internal electrode. There have been numerous studies undertaken to avoid the formation of sintering defects or to reduce the mismatch [7–10]. Usually, when the Ni paste used as an internal electrode is printed on the green sheet prepared by the so-called slot-die method used in industry, a dielectric material, $BaTiO_3$, is added into the paste to control the shrinkage mismatch. However, the shrinkage behavior will change as the powder size is reduced to reduce the layer thickness in both the dielectric and internal electrode layers. In addition, the formation of an interdiffusion layer between the dielectric and internal electrode layers has been reported in previous studies [11–14], which plays an important role in the properties of MLCCs such as dielectric constant and Curie temperature. Low sintering temperatures and compositional gradients have been recommended to decrease the interdiffusion [13]. Investigation for the interaction between the matrix, Ni, and the additive, $BaTiO_3$, in the internal electrode, however, has been limited and results here are different to those previously reported [15–17]. Therefore, estimation of shrinkage behavior and investigation of diffusion phenomena with

* Corresponding author. Tel.: +82 55 289 7201; fax: +82 55 262 6486.
E-mail address: jungyg@changwon.ac.kr (Y.-G. Jung).

0272-8842/$34.00
doi:10.1016/j.ceramint.2007.04.010

respect to the mixing composition ratio of Ni and $BaTiO_3$ powders are essential for improving reliability through the optimized fabrication process of MLCCs.

The aim of this study is to find the optimum-mixing ratio of Ni and $BaTiO_3$ powders and to know the effects of Ni and $BaTiO_3$ particle sizes on shrinkage behavior and composition change. Therefore, the present work describes the influence of the particle size of the starting materials and mixing ratio on the shrinkage behavior and interdiffusion phenomena in $BaTiO_3$-added Ni electrodes. The relationships among the starting materials, shrinkage behavior, mechanical properties, and diffusion phenomena have also been investigated.

2. Experimental procedure

Two kinds of nickel (Ni) and barium titanate ($BaTiO_3$, Sakai Chemical Industry Co. Ltd., Japan, hereinafter referred to as BT) powders were used as the matrix and additive, respectively, to modify the internal electrode in MLCCs. For the Ni powders, one was bimodal with particle sizes of 0.1 and 0.5 μm (nominal particle size of 0.3 ± 0.2 μm, Shoei Chemical Industry Co. Ltd., Japan, hereinafter referred to as Ni-1) and the other was monomodal with a particle size of 0.2 μm (Soho Chemical Industry Co. Ltd., Japan, hereinafter referred to as Ni-2). The $BaTiO_3$ powers had monomodal particle sizes of 0.1 μm (hereinafter referred to as BT-1) and 0.2 μm (hereinafter referred to as BT-2). Images observed with a scanning electron microscope (SEM, S2700, Hitachi, Japan) are shown in Fig. 1. The powders of Ni and BT were mixed in volume ratios of 90:10, 80:20 and 70:30, respectively, considering the particle sizes of Ni and BT, and reference specimens using only Ni and BT were also prepared. The mixed powders were ball-milled over 12 h in isopropyl alcohol without organic binder. Green compacts were uniaxially formed from granulated powders at 5 MPa and then hydrostatically pressed under 200 MPa. The sintering process was carried out in the reducing atmosphere of (97)Ar–(3)H_2 (vol.%) with a wet atmosphere (25 °C, H_2O), $P_{O_2} \approx 10^{-11}$ to 10^{-19}, from 700 to 1300 °C at 5 °C/min with a 150 °C interval. In each case, the dwell time was given as 1 h.

The green and sintered densities were measured for each mixing ratio, using the dimensions and Archimedes' methods after preparing the green body and at final sintering temperature, respectively. The volume shrinkage of each monolith material, the Ni and BT reference specimens, and each composite was measured in the range of 700–1300 °C at 150 °C intervals using the dimension method. The linear shrinkage of reference specimens and composites was measured with a heating rate of 5 °C/min to 1300 °C, using a dilatometer (Dilatometer, 5000S, Mac Science, Japan). Nanoindentation tests were conducted on each component: Ni matrix, BT additive, and Ni/BT interface regions in a composite, with a volume ratio of 70:30 of Ni and BT, respectively, to determine the values of elastic modulus (E) and hardness (H), using a nanoindentor (Nanoinstruments, MTS

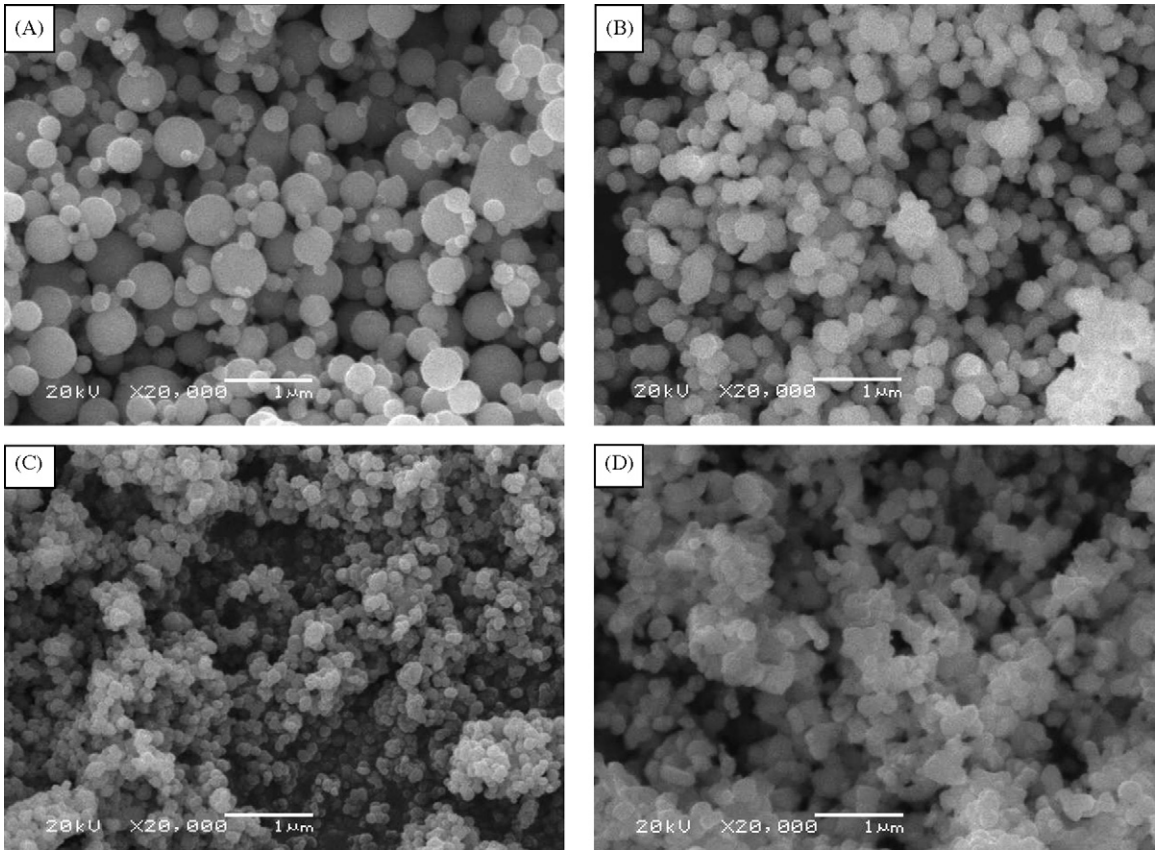

Fig. 1. SEM images of starting materials: (A and B) Ni powders of 0.3 ± 0.2 and 0.2 μm, respectively, and (C and D) $BaTiO_3$ powders of 0.1 and 0.2 μm, respectively.

Systems Corp., Eden Prairie, USA) with a Berkovich tip (tip radius <100 nm). The interfaces of the composites with 90:10 and 70:30 volume ratios were investigated using high-resolution transmission electron microscopy (HRTEM, Hitachi H-9000 NAR, Japan) to evaluate the diffusion of Ni or BT into the countergrain, in which line profile and element analyses were performed using an energy dispersive X-ray spectrometer (EDX, Hitachi H-9000 NAR, Japan).

3. Results and discussion

The volume and linear shrinkage behaviors of starting materials with different particle sizes of Ni and BT are shown in Fig. 2, as a function of sintering temperature. The volume shrinkage was measured in the range from 700 to 1300 °C at 150 °C intervals with a dwell time of 1 h at each measuring temperature, and the linear shrinkage was measured in situ during sintering with a heating rate of 5 °C/min to 1300 °C. In the case of Ni, the volume shrinkage linearly increased with increasing temperature, showing a large shrinkage at the relatively low temperature of 700 °C. The Ni of 0.3 ± 0.2 μm, Ni-1, shows less shrinkage in all ranges than the Ni with a monomodal particle size of 0.2 μm, Ni-2. The linear shrinkage of Ni-2 starts early, compared to that of Ni-1. In the case of BT, significant volume shrinkage starts from 850 °C in both BT specimens, with only a modest increase to 850 °C, while the linear shrinkage shows different starting temperatures of about 900 °C for BT-2 and about 1000 °C for BT-1. The difference in volume shrinkage between BT-1 and BT-2 increases with temperature, showing more shrinkage in the case of BT-2. Even though the starting temperature for shrinkage and the shrinkage amount with temperature are not exactly matched between isothermal and in situ data sets, the behaviors observed are quite similar.

The different shrinkage amounts and starting temperatures may be related to the relative packing densities of the green bodies, estimated as ≈60% for Ni-1, ≈48% for Ni-2, ≈61% for BT-1, and ≈52% for BT-2, even though full densification is achieved at 1300 °C in all cases. The final shrinkages between Ni-2 and BT-2 with the same particle size in both shrinkage modes are similar, with 7–8% in the linear mode and 18–19% in the volume mode, whereas their behaviors with temperature are quite different. In comparing Ni-1 and BT-1, both properties of the final shrinkage and their behavior with temperature are quite different in both shrinkage modes. The mismatch in shrinkage behavior and amount causes sintering defects such as cracking and delamination during the sintering process or in service [9,18]. The shrinkage difference or behavior is controlled by several approaches, such as adding a second phase [19], applying additional external pressure [8], or mixing binary Ni powers [20]. In this study, to overcome the difference in shrinkage behavior between the Ni internal electrode and BT dielectric layers, the addition of BT powder to Ni powder was carried out with a volume ratio ranging from 10 to 30%, which might cause constrained sintering of the Ni particles.

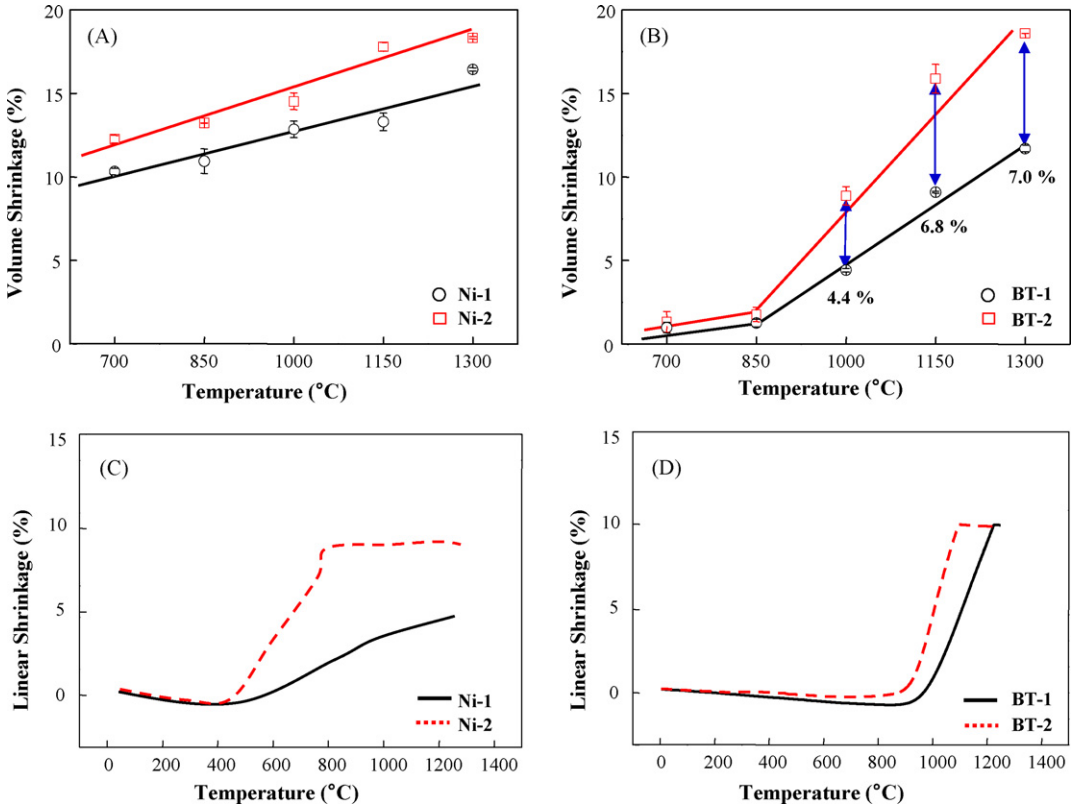

Fig. 2. Volume shrinkages of (A) Ni specimens and (B) BT specimens, and linear shrinkages of (C) Ni specimens and (D) BT specimens, as a function of sintering temperature. Volume shrinkage was measured by Archimedes' method at each temperature and linear shrinkage was obtained by in situ shrinkage measurement during sintering. Solid curves of (A) and (B) are empirical fits.

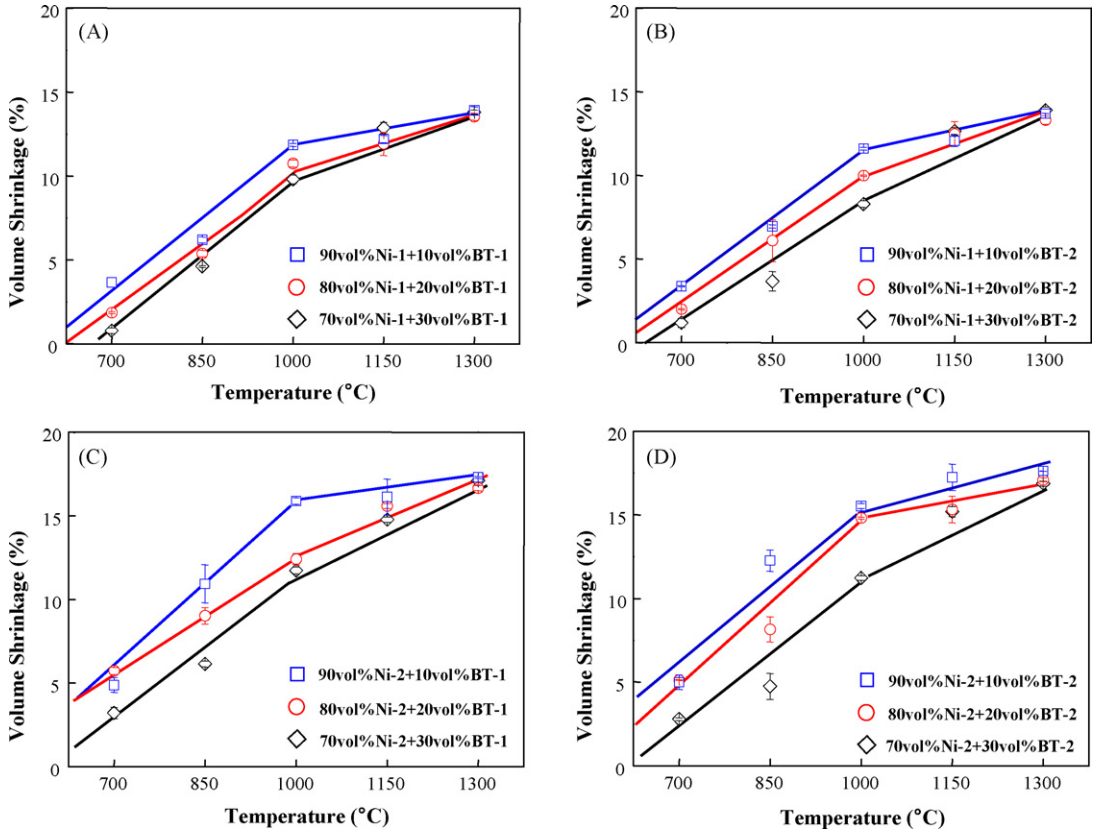

Fig. 3. Volume shrinkages of each composite with different volume ratios of Ni and BT powders, as a function of sintering temperature: (A) composites of Ni-1 and BT-1, (B) Ni-1 and BT-2, (C) Ni-2 and BT-1, and (D) Ni-2 and BT-2. Solid curves are empirical fits.

The results of volume shrinkage measured at each temperature for each composition are shown in Fig. 3, and the shrinkage in each composite at the final temperature, 1300 °C, is listed in Table 1. The shrinkage behavior changes with increasing additional amounts of BT powder to Ni powder, showing less shrinkage in all cases. However, the final shrinkage is not significantly changed with particle size and additional amount of BT: the mean shrinkage of Ni-1 composites with BT-1 and BT-2 is 13.6 and 13.2%, respectively, and of Ni-2 composites is 17.2 and 17.0%, respectively. This indicates that the matrix, Ni, is the dominant factor for the volume shrinkage, showing more shrinkage in Ni-2 composites than Ni-1 composites. However, for the linear shrinkage measured in situ during sintering, effects of particle size in both starting materials, Ni and BT, on the shrinkage behavior and amount are observed as shown in Fig. 4, without an effect of additional amounts of BT on the final shrinkage.

There are still mismatches between the monolith BT and the Ni-1 composites in both the starting temperature and shrinkage behavior, when the additional amount of BT additive is relatively small, such as 10 vol.%. The Ni-2 composite with BT-2 shows similar shrinkage behavior with BT specimens, as shown in Figs.

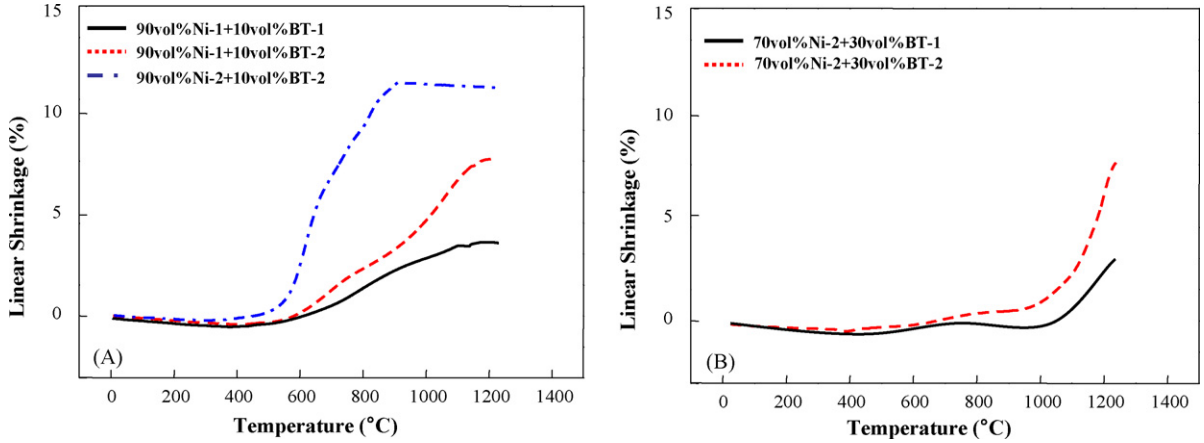

Fig. 4. Linear shrinkages of (A) 90 vol.% Ni:10 vol.% BT composites and (B) 70 vol.% Ni:30 vol.% BT composites, with different particle sizes of Ni and BT, as a function of sintering temperature.

Table 1
Comparison of shrinkage at each volume ratio

Additive	Matrix		
	Ni-1 90 vol.%; Ni-2 90 vol.%	Ni-1 80 vol.%; Ni-2 80 vol.%	Ni-1 70 vol.%; Ni-2 70 vol.%
BT-1	13.7; 17.6	13.3; 17.1	13.9; 16.9
BT-2	12.3; 17.3	13.5; 16.7	13.8; 17.1

Table 2
Elastic modulus (E) and hardness (H), at each position in Ni composites with 30 vol.% BT additive, measured using the nanoindentation technique

Property	Position		
	Ni matrix	BT additive	Ni/BT interface
E	144.4 ± 29.7	194.64 ± 7.5	175.8 ± 27.5
H	1.3 ± 0.2	4.5 ± 1.2	1.9 ± 0.2

2(D) and 4(A). The different starting temperature of shrinkage indicated between the Ni-2 composites and BT specimens is controlled by increasing the additional amount of BT powder to 30 vol.%, showing good matching in both shrinkage behavior and final shrinkage between the composite of 70 vol.% Ni-2:30 vol.% BT-2 and the monolith BT-1. Therefore, if relatively small particles of BT are used in the dielectric layer, relatively large Ni particles with large amounts of relatively large BT particles in the internal electrode layer are suggested to control the shrinkage mismatch in MLCCs during the sintering process.

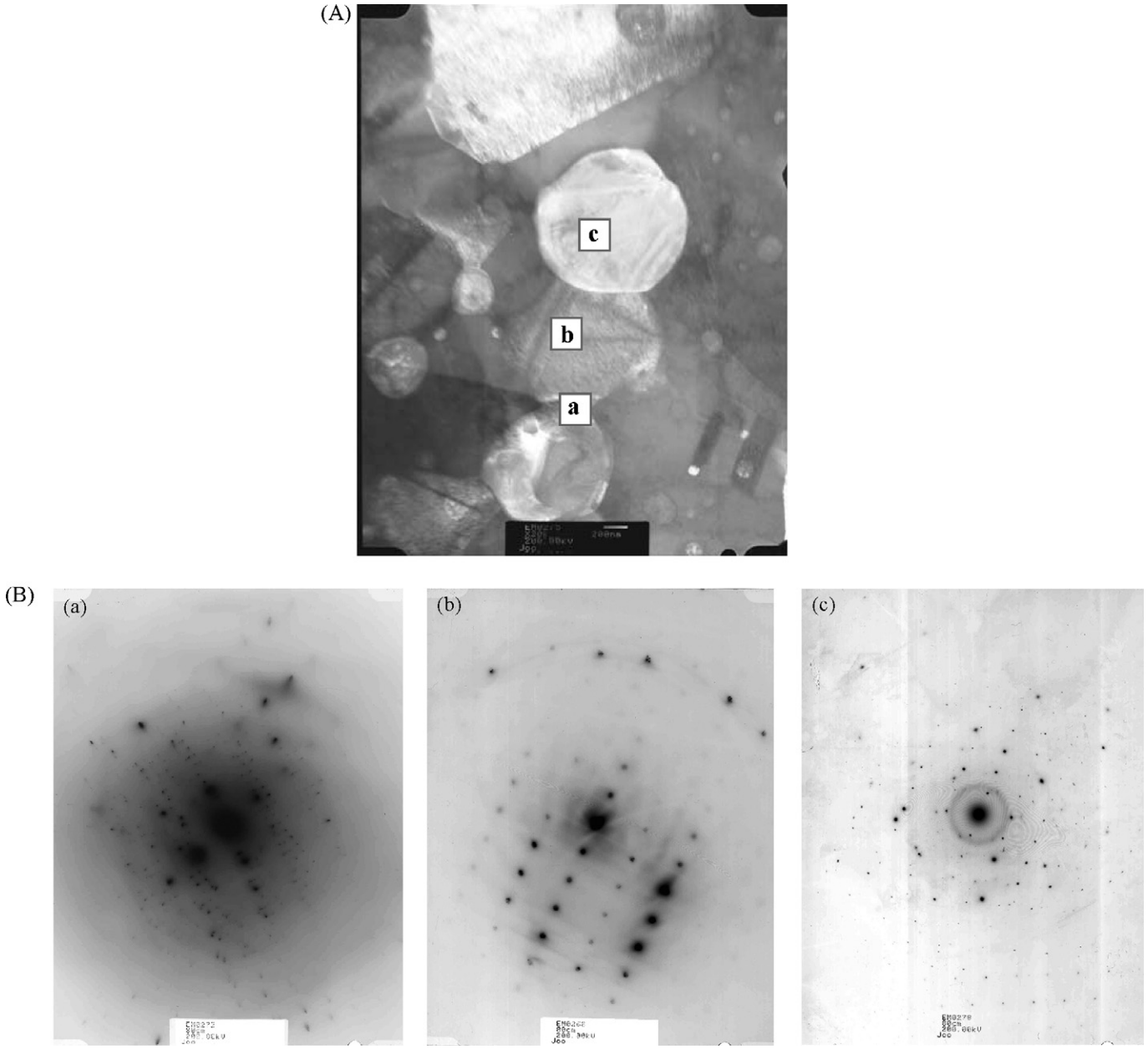

Fig. 5. TEM analysis for 90 vol.% Ni-1:10 vol.% BT-2 composite: (A) bright field TEM image, (B) diffraction patterns, and (C) EDX analysis. The interface of Ni-1 and BT-1, Ni-1 particle, and BT particle are marked as (a), (b), and (c) in Fig. 5(B and C), respectively.

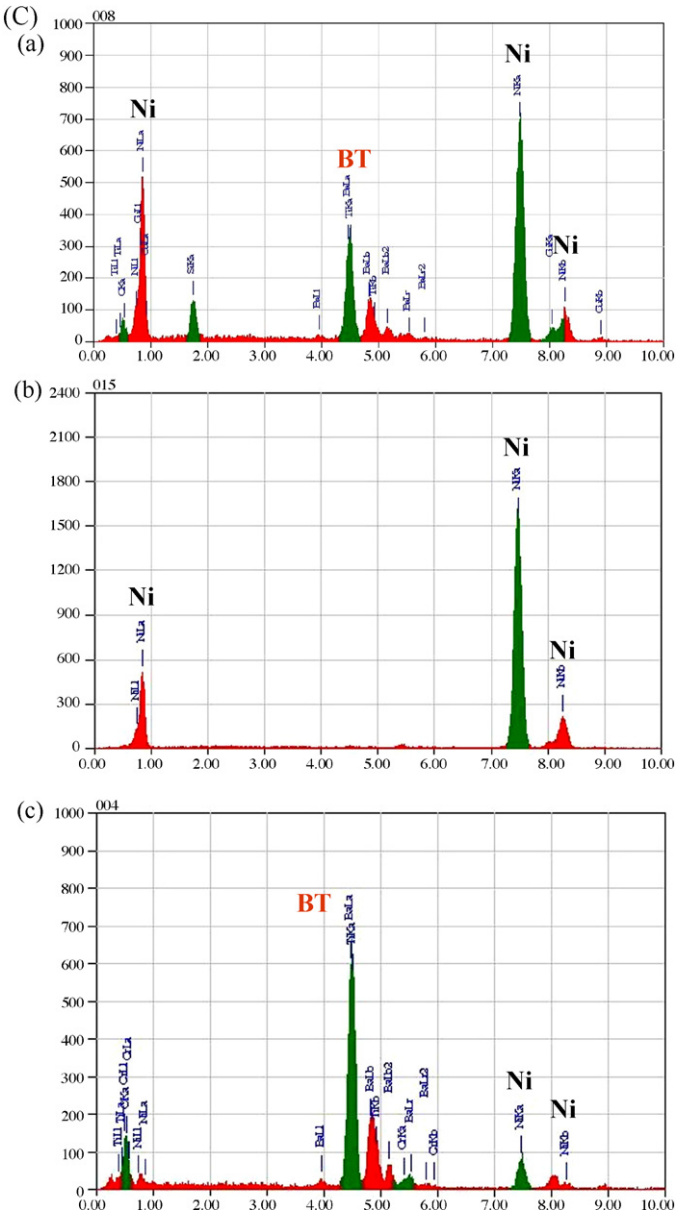

Fig. 5. (*Continued*).

Ni nanoparticles have been added into the dielectric layer to improve the dielectric properties of MLCCs, as they increase the dielectric constant but decrease the relative density, due to the increased Ni cluster size with increasing Ni content [21]. In our study, when BT powder adds up to 30 vol.% into the Ni, full densification is achieved. The mechanical properties E and H, measured by a nanoindenter, are shown in Table 2 for regions of Ni matrix, BT additive, and Ni/BT interface. The E and H values of Ni and BT measured in this study are 144.4 ± 29.7 and 1.3 ± 0.2 GPa for the Ni matrix, and 194.6 ± 7.5 and 4.5 ± 1.2 GPa for the BT additive, respectively. Reported E and H values for monolith materials are 200 and 2.4 GPa for Ni, and 125 and 10.4 GPa for BT [22–24]. From this result, it can be considered that the composition of Ni and BT will be changed by interaction between the two phases. In the interface, intermediate values are obtained, without a sudden change.

In Chen's study, the reaction between $BaTiO_3$ and Ni during the sintering process was not reported [21]. However, in other studies, diffusion phenomena of Ni from the internal electrode into the dielectric layer have been reported, in which the interdiffusion region formed near the internal electrode is hundreds of nanometers in thickness [11–13]. In Yang's studies, the interfacial reaction between Ni and $BaTiO_3$ has been affected by local oxygen activity [15–17]. Organic binders to prepare samples were used in the previous studies, which need a burnout process to remove the binders and should consider the residual carbon. However, in this study, organic binder was not added in the preparing step for preventing residual carbon and Ni oxidation during sintering.

The diffusion of elemental Ni into $BaTiO_3$ particles is observed for selected composites. The TEM results are shown in Figs. 5 and 6, and EDX results for each position in Figs. 5 and 6 are indicated in Tables 3 and 4, respectively. TEM analysis for the 90 vol.% Ni-1:10 vol.% BT-2 composite was carried out in regions of the interface between Ni and BT, Ni particle, and BT particle. In the interface marked (a) in Fig. 5, both phases of Ni and BT (Ba and Ti phases) are observed. Only the Ni phase is detected in the Ni particle marked (b) in Fig. 5, whereas both Ni and BT phases are observed inside the BT particle marked (c) in Fig. 5. However, counterdiffusion of the BT element into the Ni is not observed. This indicates that the Ni diffuses into the BT. The quantitative amount of Ni diffused into the BT is shown in Table 3. Ni phase of 9.98 mass% is detected in the BT, without another phase seen in the Ni.

When the additional amount of BT is increased to 30 vol.% and the particle size of the BT added is decreased to 0.1 μm (BT-1), Ni diffusion is also observed as shown in Fig. 6. The interdiffusion region is about 300 nm wide, and the quantitative amount is 6.48 mass% (Table 4) at point (c) of Fig. 6. Even though the Ba phase is seen at point (a), it can be disregarded as within the error range of the EDX analysis. The amount of diffusion of Ni into the BT increases as the particle size of the BT added into the Ni matrix increases, indicating that the particle size mainly affects the diffusion behavior of elemental Ni, without the additional effect of the volume ratio. The interdiffusion region observed, in this study, is smaller than the previously reported one, in which an interdiffusion region of about 1400 nm between the internal electrode and dielectric

Table 3
EDX results at each position in Fig. 4 for Ni-1 and BT-2 composite with 90:10 volume ratio

Element (keV)	Point analysis					
	Position (a)		Position (b)		Position (c)	
	Mass (%)	Atom (%)	Mass (%)	Atom (%)	Mass (%)	Atom (%)
O K	39.65	–	–	–	19.08	–
Ti K(4.508)	2.07	3.06	–	–	14.68	34.60
Ni K(7.471)	12.69	15.32	100	100	9.98	19.18
Ba L(4.464)	16.27	8.40	–	–	56.26	46.23
Total	–	–	100	100	100	100

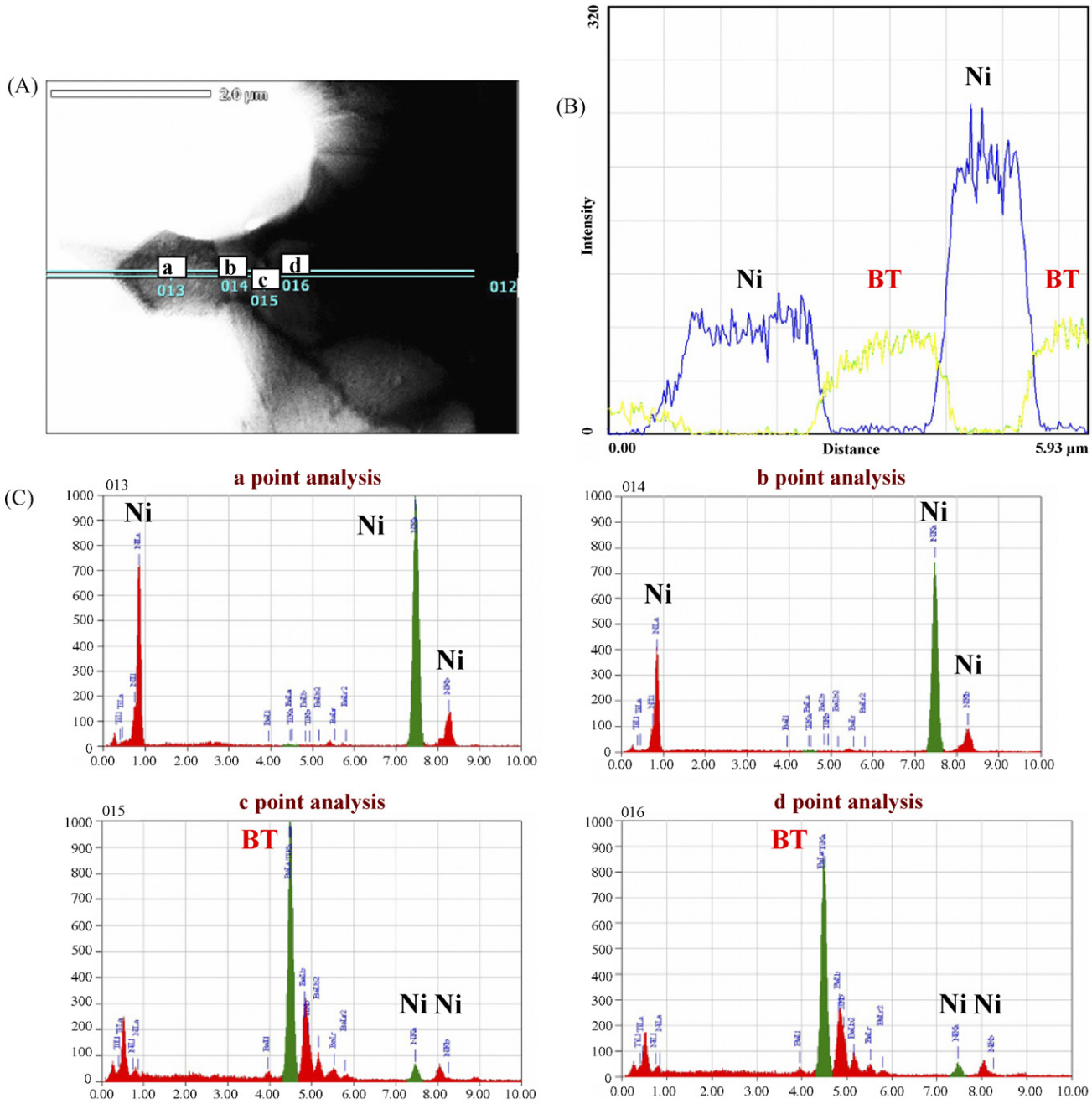

Fig. 6. TEM analysis for 70 vol.% Ni-1:30 vol.% BT-1 composite: (A) TEM image, (B) line spectra analysis, and (C) EDX analysis.

Table 4
EDX results at each position in Fig. 5 for Ni-1 and BT-1 composite with 70:30 volume ratio

Element (keV)	Point analysis							
	Position (a)		Position (b)		Position (c)		Position (d)	
	Mass (%)	Atom (%)	Mass (%)	Atom (%)	Mass (%)	Atom (%)	Mass (%)	Atom (%)
Ti K(4.508)	–	–	0.41	0.5	18.05	36.35	18.05	36.70
Ni K(7.471)	99.27	99.69	99.59	99.5	6.48	10.64	5.46	9.06
Ba L(4.464)	0.73	0.31	–	–	75.47	53	76.49	54.24
Total	100	100	100	100	100	100	100	100

layers was reported [11,12]. However, in our study, interdiffusion within the internal electrode layer is considered. Therefore, the quantitative amount of diffusion and the size of the interdiffusion region cannot be matched with the previous study. Even though elemental diffusion has advantages in enhancing the mechanical strength and improving the breakdown resistance of multilayer components, excess diffusion or incorporation can deteriorate the reliability and aging resistance of MLCCs, due to the formation of some lattice defects, oxygen vacancies, and the like [13–17]. Therefore, in the Ni and BT system, when two materials are used to prepare a layered structure or composite, the interdiffusion of elemental Ni into BT particles or the dielectric layer should be considered and controlled.

4. Conclusions

The shrinkage behavior and interfacial diffusion phenomena of Ni-based composites as a function of particle size of starting materials and additional amounts of BT additives have been investigated for the application of Ni-based internal electrodes in MLCCs. The particle sizes of Ni and BT affect the relative packing density, resulting in smaller amounts of shrinkage for small particle sizes, except the monolith BT. The shrinkage behavior is changed with additional amounts of BT added into Ni, and the shrinkage of Ni composites gradually decreases with an increase in the additional amount of BT, without an effect on the final shrinkage. The different starting temperature of shrinkage is controlled by increasing the additional amount of BT powders to 30 vol.%, showing good matching in the shrinkage behavior and final shrinkage between the composite of 70 vol.% Ni-2:30 vol.% BT-2 and the monolith BT-1. In the TEM and EDX studies on Ni composites, elemental Ni diffuses into the BT particle without counterdiffusion from BT to Ni. The Ni phase is detected inside the BT particle for the composite with 90 vol.% Ni-1:10 vol.% BT-2, whereas the interdiffusion region is about 300 nm for the composite with 70 vol.% Ni-1:30 vol.% BT-1. The amount of diffusion is affected by the particle size of the BT added, rather than the amount added. The composition change in the Ni matrix and the BT additive due to interdiffusion affects the mechanical properties, E and H, at each position in the Ni composites.

Acknowledgment

This work was financially supported by the Korea Research Foundation (KRF-2004-005-D00111).

References

[1] T. Nomura, T. Kato, Y. Nagano, in: Proceedings of the 9th US–Japan Seminar on Dielectric and Piezoelectric Ceramics, 1999, pp. 295–298.
[2] T. Tsurumi, Y. Yamanoto, N. Ohashi, H. Chazono, Y. Inomata, H. Kishi, in: Proceedings of the 9th US–Japan Seminar on Dielectric and Piezoelectric Ceramics, 1999, p. 345.
[3] Y. Sakabe, Dielectric materials for base-metal multilayer ceramic capacitors, Am. Ceram. Soc. Bull. 66 (1987) 1338–1341.
[4] J. Yamamatsu, N. Kawno, T. Arashi, A. Sato, Y. Nakano, T. Nomura, Reliability of multilayer ceramic capacitors with nickel electrodes, J. Power Sources 60 (1996) 199–203.
[5] D.F.K. Hennings, Dielectric materials for sintering in reducing atmosphere, J. Euro. Ceram. Soc. 21 (2001) 1637–1642.
[6] N. Halder, D. Chattopadhyay, A.D. Sharma, D. Saha, A. Sen, H.S. Maiti, Effect of sintering atmosphere on the dielectric properties of barium titanate based capacitors, Mater. Res. Bull. 36 (1991) 905–913.
[7] U. Paik, K.M. Kang, Y.G. Jung, J. Kim, Binder removal and microstructure with burnout condition in $BaTiO_3$ based Ni-MLCCs, Ceram. Inter. 29 (2003) 939–946.
[8] D.H. Park, Y.G. Jung, U. Paik, Crack suppression behavior with post-process parameters in $BaTiO_3$ based Ni-MLCCs, Ceram. Inter. 31 (2005) 655–661.
[9] R.K. Bordia, G.W. Scherrer, On constrained sintering—I. Constitutive model for a sintering body, Acta Metall. 36 (9) (1988) 2393–2397.
[10] Y. Kinemuchi, S. Uchimura, K. Watari, Centrifugal sintering $BaTiO_3$/Ni layered ceramics, J. Europ. Ceram. Soc. 25 (2005) 2223–2226.
[11] Y. Wang, L. Li, J. Qi, Z. Ma, J. Cao, Z. Gui, Nickel diffusion in base metal electrode MLCCs, Mater. Sci. Eng. B 99 (2003) 378–381.
[12] Z.L. Gui, Y.L. Wang, L.T. Li, Study on the interdiffusion in base-metal-electrode MLCCs, Ceram. Inter. 30 (2004) 1275–1278.
[13] R. Zuo, L. Li, Y. Tang, Z. Gui, Characteristics and effects of interfacial interdiffusion in composite multilayer ceramic capacitors, Mater. Chem. Phy. 69 (2001) 230–235.
[14] S. Sumita, M. Ikeda, Y. Nakano, Degradation of multilayer ceramic capacitors with nickel electrodes, J. Am. Ceram. Soc. 74 (1994) 2739–2746.
[15] G.Y. Yang, S.I. Lee, Z.J. Liu, C.J. Anthony, E.C. Dickey, Z.K. Liu, C.A. Randall, Effect of local oxygen activity on Ni–$BaTiO_3$ interfacial reactions, Acta Meter. 54 (2006) 3513–3523.
[16] G.Y. Yang, E.C. Dickey, C.A. Randall, D.E. Rarber, P. Pinceloup, M.A. Henderson, R.A. Hill, J.J. Beeson, D.J. Skamser, Oxygen nonstoichiometry and dielectric evolution of $BaTiO_3$. Part I—improvement of insulation resistance with reoxidation, J. Appl. Phys. 96 (2004) 7492–7499.
[17] G.Y. Yang, G.D. Lian, E.C. Dickey, C.A. Randall, D.E. Rarber, P. Pinceloup, M.A. Henderson, R.A. Hill, J.J. Beeson, D.J. Skamser, Oxygen nonstoichiometry and dielectric evolution of $BaTiO_3$. Part II—insulation resistance degradation under applied dc bias, J. Appl. Phys. 96 (2004) 7500–7508.
[18] R.K. Bordia, R. Raj, Sintering behavior of ceramic films constrained by a rigid substrate, J. Am. Ceram. Soc. 68 (6) (1985) 287–292.
[19] P.Z. Cai, D.J. Green, G.L. Messing, Constrained densification on alumina/zirconia hybrid laminates, I: experimental observation of processing defects, J. Am. Ceram. Soc. 80 (8) (1997) 1929–1939.
[20] D.H. Im, S.H. Hyun, S.Y. Park, B.Y. Lee, Y.H. Kim, Preparation of Ni paste using binary powder mixture for thick film electrodes, Mater. Chem. Phys. 96 (2006) 228–233.
[21] R. Chen, X. Wang, H. Wen, L. Li, Z. Gui, Enhancement of dielectric properties by additions of Ni nano-particles to a X7R-type barium titanate ceramic matrix, Ceram. Inter. 30 (2004) 1271–1274.
[22] G.S. White, C. Nguyen, R. Rawal, Young's modulus and thermal diffusivity measurements of barium titanate based dielectric ceramics, in: In Proceedings of Nondestructive Testing of High Performance Ceramics, 1987, pp. 371–379.
[23] D.R. Lide, CRC Handbook of Chemistry and Physics, 85th ed., CRC Press, Boca Raton, London, New York, Washington, DC, 2004–2005.
[24] R.A. Mirshama, P. Parakala, Nanoindentation of nanocrystalline Ni with geometrically different indenters, Mater. Sci. Eng. A 372 (2004) 252–260.